**Journal of Magnetics** 2(4), 116-122 (1997)

# A Study of Co, Ni, Mn, and Al Containing Goethites by Mössbauer Spectroscopy

**Eng Chan Kim, Hyeun Gook Hwang and Yong Soon Hwang**

*Department of Physics, Yeungnam University, Gyongsan 712-749, Korea*

**Jung Gi Kim**

*Department of Physics, Hanyang University, Seoul 133-791, Korea*

**V. I. Nikolaev**

*General Physics Department, Moscow State University, Moscow 117234, Russia*

(Received 8 September 1997)

**To determine whether there is an ionic substitution of Ni, Co, Mn, and Al for Fe in synthetic goethites these materials have been studied by Mössbauer spectroscopy at various temperatures ranging from 77 to 400 K. It is found that the presence of substituting elements in magnetically ordered structure of crystals may change the shape of Mössbauer spectra of these materials. The approximate distribution function of the effective magnetic field in the Fe nucleus $\rho(Hn)$ is obtained from the Mössbauer spectra. It is noted that the mean value of $\rho(Hn)$ and its integral width can be taken as a measure of substitution in goethites.**

## 1. Introduction

Goethite ($\alpha$-FeOOH) is one of the major materials in oxide nickeliferrous ores. Since it is a Ni, Co, Mn, and Al bearing minerals, it is important for geology and for extractive technology [1-5] to know what is the type of association between these metals and the oxy-hydroxide. Goethites are antiferromagnetic below the Néel temperature ($T_N$ = 393 K).

The presence of substituting elements in magnetically ordered structure of crystals may change the shape of Mössbauer spectra of these materials. The purpose of this study is to determine whether there is an ionic substitution of Ni, Co, Mn, and Al for Fe in synthetic goethites.

## 2. Computational Procedure

Consider an experimental Mössbauer spectrum $S(x)$ which consists of a superposition of contributions from elementary spectra. Each elementary spectrum is-apart from trivial constants-given as a function of two variables, the energy (the Channel-number) $x$ and one (continuously varying) additional parameter $y$, which conveniently could be thought of as one of the hyperfine parameters. Other variables that may be necessary to define the spectrum will not be considered at this point and are therefore not specified explicitly. Each of these elementary spectra represented by the experssion $A(x, y)$ should be weighted relatively with a weight-factor $F(y)$, thus superimposing into the analytic expression

$$G(x) = \int_{y_1}^{y_2} F(y)\ A(x, y)\, dy \tag{1}$$

where the limits $y_1$ and $y_2$ reflect the assumption that $F(y)$ is non-zero only in a limited interval. The expression $A(x, y)$ contains all basic information about the elementary spectra, such as line-width, possible symmetries etc, and it is assumed in the following that this information is known.

The equation to be solved thus becomes

$$S(x) + \varepsilon(x) = \int_{y_1}^{y_2} F(y)\ A(x, y)\, dy \tag{2}$$

where the error term $\varepsilon(x)$ reflects that the experimental spectrum $S(x)$ will always differ from the analytical experssion $G(x)$ because of, for example, counting statistics. In order to solve numerically equation (2) we make a matrix approximation. The interval from $y_1$ and $y_2$ is subdivided into N parts, and the integral equation (2) is then replaced by the linear system

$$S_i + \varepsilon_i \sum_{j=1}^{N} f_j\, a_{ij} \tag{3}$$

© 1997 The Korean Magnetics Society

or in matrix form

$$S + \varepsilon = AF \tag{4}$$

Following Phillips [6], this equation can be solved under the constraints that the sum of squares of errors ($\sum i\varepsilon_i^2$) is minimised, while at the same time minimising the sum of squares of second differences ($\sum j d_j^2$) of $F$ : the latter is equvialent to demanding a certain degree of smoothness of $F$ by minimising a trend towards local linearity by imposing the expression

$$\sum_j d_j^2 \equiv \sum_j [(f_{j+1} - f_j) - (f_j - f_{j-1})]^2 = \sum_j (f_{j+1} - 2f_j - f_{j-1})^2 \tag{5}$$

These two requirements cannot be fulfilled simultaneously, but must be weighted relatively by employing a Lagrangian multiplier, $\gamma$, so that the expression $U$ to be minimised becomes:

$$U \equiv \gamma \sum_j (f_{j+1} - 2f_j + f_{j-1})^2 + \sum_j \varepsilon_i^2 \tag{6}$$

From this expression proposed by Phillips (1962) [6] and Twomey (1963) [7] the distribution function $F$ may be determined.

The distribution function $F$ can often be considered finite in a limited interval only, and the interval chosen for the calculations must include at least this interval. However, when this requirement is fulfilled, the distribution function should have zero (or close to zero) values at the end-points ( j = 1 and j = N). However this fundamental requirement is, in general not fulfilled by the distribution function obtained by minimising the expression (6), and in practice the intensities at the end-points are quite often found to display large positive - or even negative-values.

This problem of improper end-pont behaviour may be solved by extending equation (6) to include the additional constraint that the end-point intensities must be close to zero. It should be recognised that this constraint is a special case of the more general one, where (at least in principle) every point in the distribution $f_j$ is subject to a trend towards a prescribed value $k_j$, imposed with individual strength defined by a Lagrangean multiplier $\beta_j$. The expression $U$ to be minimised then becomes;

$$U \equiv \gamma \sum_j (f_{j+1} - 2f_j + f_{j-1})^2 + \gamma \sum_j \beta_j (f_j - k_j)^2 + \sum_i \varepsilon_i^2 \tag{7}$$

Minimising with respect to $f_j$ one finds

$$\frac{\partial U}{\partial f_j} = 2\gamma(f_{j-2} - 4f_{j-1} + (6+\beta_j) f_j - 4f_{j+1} + f_{j+2}) + 2\sum_i \varepsilon_i a_{ij} - 2\gamma \beta_j k_j = 0 \tag{8}$$

Defining a matrix H with the elements

$$h_{ij} = \delta_{i-2,j} - 4\delta_{i-1,j} + 6\delta_{ij} - 4\delta_{i+1,j} + \delta_{i+2,j} \tag{9}$$

where $\delta_{ij}$ is the Kronecker delta, and $\delta_{ij} = 0$ for $i < 1$ and $i > N$, equation (8) may be written.

$$\gamma(H + B) F + A^+ \varepsilon - \gamma B K = 0 \tag{10}$$

where $A^+$ is the transpose of A and B is a diagonal matrix with $b_{ij} = \beta_j$. By use of equation (4) we obtain

$$(A^+ A + \gamma H + \gamma B) F = A^+ S + \gamma B K \tag{11}$$

This expression can be greatly simplified for our purpose. Since we bind only the end-points, all $\beta_j$'s are equal to zero, except $\beta_1$ and $\beta_N$, and since we want constraint to the zero, K is the null vector.

Thus, equation (11) can be reduced to:

$$(A^+ A + \gamma R) F = A^+ S \tag{12}$$

where the matrix elements of R are given by $r_{11} = h_{11} + \beta_1$, $r_{NN} = h_{NN} + \beta_N$, and for all other $(i, j)$, $r_{ij} = h_{ij}$.

In addition it should be mentioned that smoothing of the second differences (as in equation (5)) can be substituted, for example by smoothing of the third differences (Twomey 1963), and in this case the distribution function is subject to a somewhat less restrictive smoothing.

For completeness it should be noted that an expression similar to equation (7) may be used to constrain the distribution function to have positive values only. This can be obtained by replacing the second-order term $(f_j - k_j)^2$ with some step function-like expression $P(f_j)$ giving a large contribution to $U$ for $f_j < 0$ and zero contribution for $f_j \geq 0$:

$$U \equiv \gamma \sum_j (f_{j+1} - 2f_j + f_{j-1})^2 + \gamma \beta \sum_j P_j(f_j) + \sum_i \varepsilon_i^2 \tag{13}$$

The possibility of avoiding negative intensities by use of nonlinear programming has been pursued by Le Caer and Dubois (1979) [8].

The proper choice of the Lagrangean multipliers $\gamma$, $\beta_1$ and $\beta_N$ depends on the details of the problem in question. In praticle the choice will ultimately rest on the estimation of how the vlaues of $\gamma$, $\beta_1$ and $\beta_N$ influecne the quality of fit, represented by $\chi^2$ or an equivalent statistical parameter. If an increase in $\gamma$ causes no essential increase in $\chi^2$ this higher value of $\gamma$ should be adapted, and those details of the distribution function that disappear upon the increased smoothig should be immaterial. The value of $\beta_1$ and $\beta_N$ too should be chosen just large enough to ensure the required end-pont behaviour without causing a significant increase in $\chi^2$.

If the spectrum S is to be interpreted in terms of two distributions rather than one, R must be broken up into a

**Journal of Magnetics**, Vol. 2, No. 4, December, 1997

two-block matrix, since smoothing must be carried out independently on the two distributions. This also means that endpoint constraint may involve four, rather than two points Equation (12) then applies for each block seperately.

Up to this point attention has been focused on the parameters that display continuous variation. However, since the interpretation of any realistic spectrum involves introduction of several free parameters, the remaining ones must be assigned definite values before applying equation (12). We then propose to determine the values of such parameters through an iteration procedure. Every step in such a procedure will involve the following major parts:

(i) construction of A form the given values of the free parameters;
(ii) determination of $F$ from $(A^{\cdot}A+\gamma R)F=A^{\cdot}S$;
(iii) construction of the generated spectrum $G=AF$;
(iv) calculation fo chi square $\chi^2\sim\sum_i(g_i-s_i)^2$

The time consuming part is step no 2. It calls for swift convergence and consequently makes heavy demands on the quality of the initial guess. The choice of iteration algorithm must be made accordingly.

## 3. Experiment

Several goethites were synthetized: first one is pure (G), second one containing Ni only (GNi), third one containing Co only (GCo), forth one containing Al only (GAl), and the last one containing all these four metals (GT).

Chemical composition of the synthetic materials is listed in Table I.

Table I. Chemical composition of the synthetic materials.

| Material | Composition (% in weight) | | | | |
|---|---|---|---|---|---|
| | Fe | Co | Ni | Mn | Al |
| G | 58.75 | | | | |
| GCo | 57.38 | 0.22 | | | |
| GNi | 57.38 | | 1.05 | | |
| GMn | 55.56 | | | 2.05 | |
| GAl | 49.48 | | | | 3.7 |
| GT | 50.79 | 0.16 | 1.04 | 1.63 | 3.9 |

The contents of these elements in the samples were similar to the average composition of that mineral in the Russian lateritic ores.

The samples were prepared in the following way: a $Fe(No_3)_3\cdot 9H_2O$ 1M solution was added to nitrate of the metals in the appropriate amount of the desired element and it was mixed slowly during stirring with an diluted solution of $NH_3$ at 25 %.

The precipitate was obtained and washed with deionized water up to neutral pH and left in a KOH 2M solution for 7 days. Afterwards, it was dried in steam for 4 hours. The precipitate thus becomes goethite from amorphous ferric oxide. To eliminate potassium hydroxides, ammonium chloride was added. The obtained product was washed up to the absence of chloride ions and dried in air for several days.

The samples was investigated by X-ray powder diffraction (XRD) using CoK$\alpha$ radiation and a Philips PW 1050 diffractometer mounted with a graphite monochromator in the diffracted beam. The sample was scanned in the range 15-90° 2$\theta$.

A Mössbauer spectrometer of the electromechanical type was used in the constant-acceleration mode. A $^{57}$Co single-line source in a rhodium matrix was used at room temperature. Sample thickeness was calculated to obtain an iron surface density of about 15 mg/cm$^2$.

Electron micrographs were obtained after ultrasonical dispersion of the sample in water using a Jeol Jem 100B microscope operating at 80 kV.

## 4. Results and Discussion

The samples have been studied by X-ray diffraction, IR spectroscopy and TEM [9]; the only phase found was goethite. According to the values obtained for the integral width of the diffractogram lines, and the position of the 640 cm$^{-1}$ band in the IR spectra, the following crystallinity of diminishing order was established: GAl, GMn, GCo, GNi, G; and from electron micrographs the following particle size of diminishing order was established: GMn, G, GNi, GCo, GAl.

Electron micrographs of samples were obatined after ultrasonical dispersion.


Fig. 1. Electron micrograph of GCo.

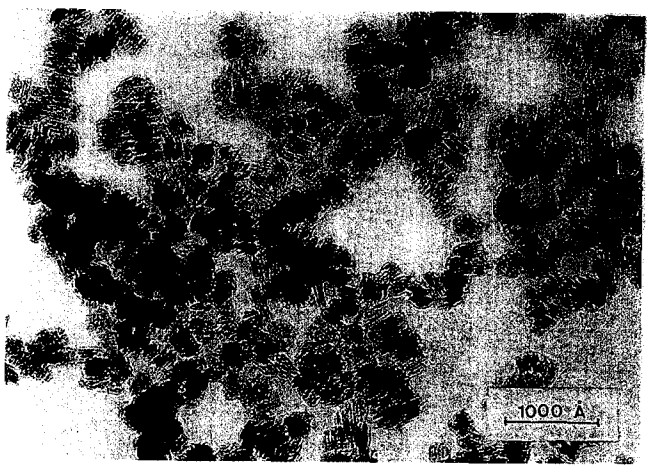


Fig. 2. Electron micrograph of GT.

Typical micrographs of GCo and GT are shown in Fig. 1 and 2. In GCo the dimensions are 300~1500 Å (length) and 120~180 Å (width). In sample GT typical dimensions of the particles are $235 \times 120 \times 40$ Å$^3$. Thus in both samples the dimensions of the particles are consistent with the dimensions of the crystallites found by use of XRD.

The XRD measurements showed that the only crystalline phase of the sample was goethite and there was no indication of any remaining armorphous phase.

From the corrected widths at half height of the diffraction lines the mean crystallite dimension, D, along different directions was calculated using the Scherrer formula, assuming that broadening is solely due to crystallite size. The calculated dimensions are given in Table II along with values of the goethites [10].

Table II. Mean crystallite dimension, D(nm), of goethite.

| | GCo | GT | Natural Sample |
|---|---|---|---|
| $D^{020}$ | 19.5 | 67.0 | 44.7 |
| $D^{110}$ | 11.0 | 69.0 | 24.9 |
| $D^{120}$ | 13.0 | 23.5 | 25.2 |
| $D^{021}$ | 23.0 | 110.0 | 51.8 |

The XRD results indicate that in the present sample the crystallographic c-axis is parallel to the long axis of the crystallites.

Mössbauer spectra of the natural goethite sample at 79, 298 and 374 K are shown in Fig. 3. The absorber was prepared with 15 mg Fe per cm$^2$, i. e., the sample effective absorber thickness as the $\alpha$-Fe calibration foil. The Mössbauer absorption lines are only slightly broader than those of the calibration foil, indicating that the sample is well crysatllized. The Mössbauer parameters of the spectra are given in Table III. The Néel temperature, $T_N$, was determined by measuring the absorption at zero source velocity as a function of temperature in the range 380 ~402 K. The result was $T_N = 393.4 \pm 0.5$ K, which is in excellent agreement with the result of Van der Woude and Dekker ($T_N = 393.3$ K) [11]. Thus the natural goethite sample seems to be well-crystallized and therefore suitable as reference sample.

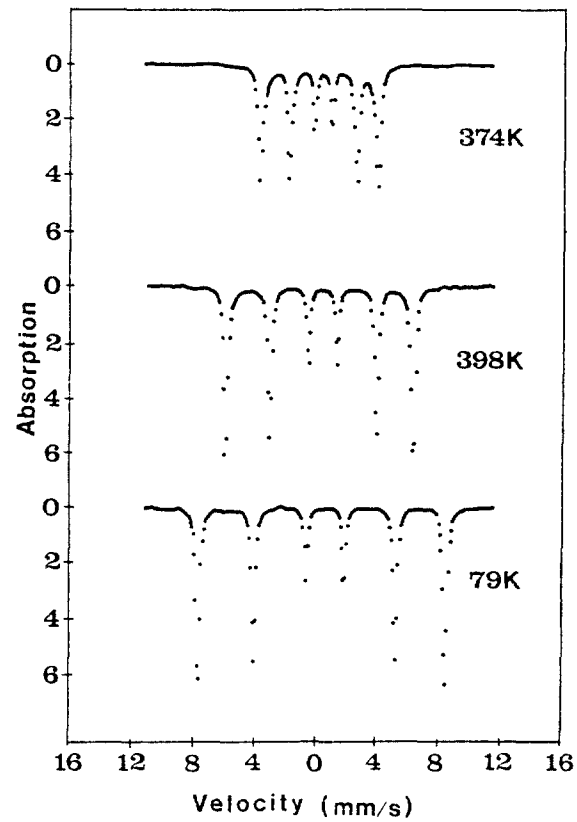


Fig. 3. Mössbauer spectra of a well-crystallized natural sample of goethite at various temperatures.

Table III. Mössbauer parameters of well-crystallized goethite.

| $T$ (K) | $\delta$ (mm/s) | $\varepsilon$ (mm/s) | $H$ (kOe) |
|---|---|---|---|
| 79 | 0.48 ± 0.01 | −0.14 ± 0.01 | 501 ± 4 |
| 298 | 0.37 ± 0.01 | −0.14 ± 0.01 | 381 ± 4 |
| 374 | 0.32 ± 0.01 | −0.12 ± 0.01 | 242 ± 4 |

Figs. 4 and 5 show spectra of GT at different temperatures. At low temperatures the spectra have relatively narrow lines, but above 130 K the lines become asymmetrically broadened in the way typical for microcrystalline goethite. Above 290 K a central doublet is present in the spectra and between 300 and 320 K the relative area of this doublet rapidly increases at the expense of the magnetically split com-

ponent (Fig. 5). The distibutions in magnetic hyperfine fields were calculated by use of the computer program developed by Wivel and Morup [12]. The quadrupole splitting constant $\varepsilon$ is $(-0.12 \pm 0.02)$ mm/s at all temperatures and the isomer shifts at 80 K is $(0.47 \pm 0.02)$ mm/s and $(0.38 \pm 0.02)$ mm/s at 298 K, i. e., within the uncertainty identical to the values for reference sample.

The spectra of the non Al containing goethites similar to the GCo spectrum, with lines showing an asymmetrical broadening and amplitudes noticeably far from the theoretical relation 3:2:1. Morup et al. [10, 13] explained the magnetic field decrease of the $\alpha$-FeOOH without substituents considering the collective magnetic excitation and the asymmetry of the lines due to the distribution of the particle size, and also taking into account the magnetic couplings between the crystals. The spectra of the goethite GAl and GT present a superparamagnetic doublet in the middle. In the case, the most important factor is the diamagnetic character of the $Al^{3+}$ cation which interrupts the superexchange chains of the hydroxide structure, responsible for the magnetic ordering.

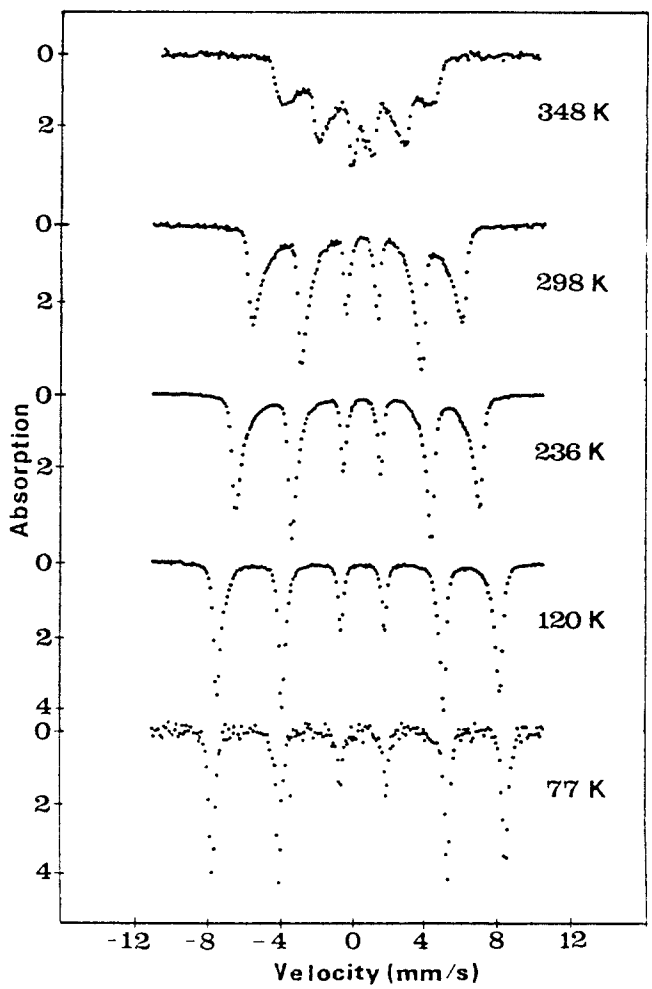


Fig. 4. Mössbauer spectra of GT below the magnetic transition temperature.

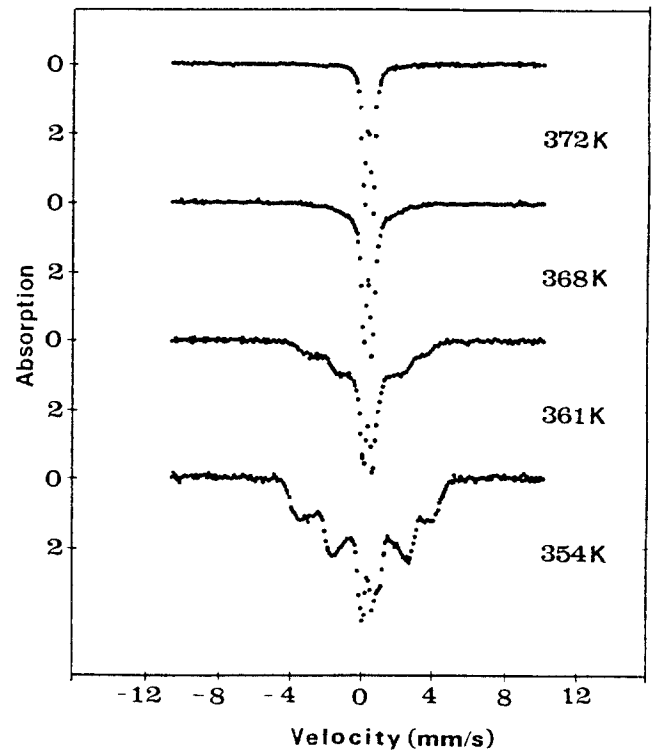


Fig. 5. Mössbauer spectra of GT in the vicinity of the magnetic transition temperature.

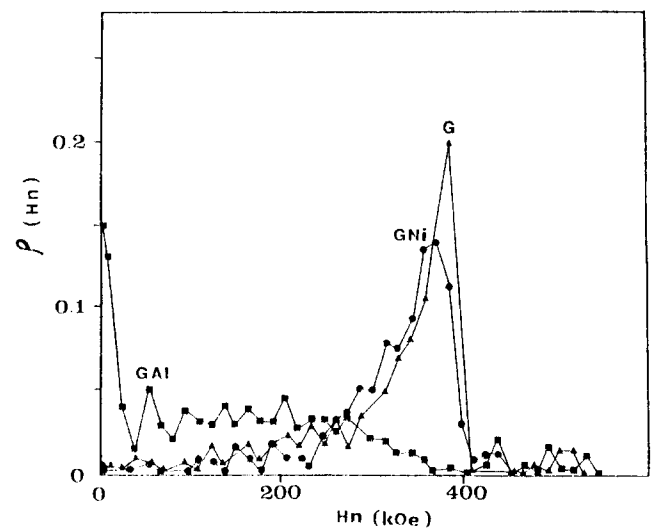


Fig. 6. Approximate effective magnetic field density distribution function at the Fe nuclei, $\rho$ ($Hn$) of the synthetic goethites.

Initially, approximate Mössbauer spectra parameters of the non Al containing goethites were obtained using least-squares computer program [14] and using them for distribution function [15, 16] data input, more refined parameter values were reached. Those parameters are shown in Table Ⅳ and the approximate distribution function of the effective magnetic field in the iron nuclei $\rho$ ($Hn$) [11] calculated from the mentioned spectra by the distribution program, is shown in Fig. 6.

Table Ⅳ. Mössbauer spectra parameters of none Al containing sythetic goethites, magnetic hyperfine field $H$, quadrupole shift $\varepsilon$, and isomer shift $\delta$ relative to iron metal.

| Goethite | $\delta$ (mm/s) | $\varepsilon$ (mm/s) | $H$ (kOe) |
|---|---|---|---|
| G | 0.39 ± 0.01 | 0.26 ± 0.01 | 332 ± 4 |
| GCo | 0.39 ± 0.01 | 0.25 ± 0.01 | 313 ± 4 |
| GNi | 0.39 ± 0.0 | 0.25 ± 0.01 | 311 ± 4 |
| GMn | 0.39 ± 0.01 | 0.25 ± 0.01 | 305 ± 4 |

It is apparent that a relation exists between the shape of the function $\rho$ ($Hn$) and the concentration of the elements added to the goethite. This relation is more clear in Fig. 7 where the variation of the average value $\overline{Hn}$ and the normalized integral width AI of the mentioned density distribution function with the concentration of the additional element in the goethite are shown. The dependency shown indicates that those parameters could be taken as a semiquantitative indicator of the substitution degree of those elements in the goethite in spite of other factors such as the crystallinity and particle size. Thus, for example, although the goethite with Mn show the larger particle size and the larger crystallinity among the non Al containing samples, it has the widest magnetic field distribution function and the lowest value of effective magnetic field.

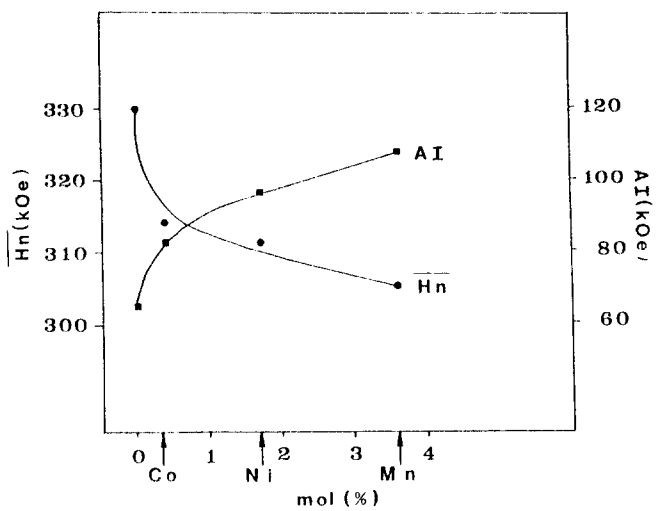


Fig. 7. Mean value $\overline{Hn}$ and the integral width AI of the effective magnetic field density distribution function at the Fe nuclei of the synthetic goethite as a function of the additional element concentration.

The shape of the function $\rho$ ($Hn$) for the goethite GAl differs from the others. The values $Hn$ and AI for this material (134 kOe and 8 kOe, respectively) do not follow the same dependency shown in Fig. 6, precisely due to the presence of the $Al^{3+}$ diamagnetic ions.

For the Al containing goethites (GAl and GT) the corresponding Mössbauer spectra at 77 K are six Lorentzeans with a slight line broadening. The values of $Hn$ and AI, calculated from these spectra together with the goethite without substituents at the same temperature (Table Ⅴ) show that also in the Al containing goethites, these parameters could be taken as semiquantative indexes of the Fe substituent degree by other elements.

Table Ⅴ. Mean value $\overline{Hn}$ and integral width AI for the effective magnetic field density distribution function at the iron nuclei for goethites G, GAl, and GT at 77 K.

| Goethite | $\overline{Hn}$ (kOe) | AI (kOe) |
|---|---|---|
| G | 470 ± 5 | 34 ± 5 |
| GAl | 464 ± 5 | 43 ± 5 |
| GT | 454 ± 5 | 46 ± 5 |

The relation of the mean values and integral width of the effective magnetic field density distribution function at the Fe nuclei with the Co, Ni, Mn, and Al concentration, in spite of the particle size distribution and crystal perfection degree, proves that these elements take part in the structure of the studied synthetic goethites substituting the Fe, indicating that they can substitute this element in the goethites of the oxidized nickel ores. Such parameters can be taken as a semiquantitative measure of the substitution degree in the goethites.

## Acknowledgements

We thank to Dr. A. V. Bykov at General Physics Department of Moscow State University for assisting us in synthesizing goethites.

This research was supported by the Yeungnam University Research Grants in 1997 and is partially supported by the Korean Ministry of Education through Research Fund Project No. BSRI-97-2447.

## References

[1] D. G. Rancourt, Nuclear Instruments and Methods in Physics Research **B58**, 85 (1889).
[2] M. D. Dyar, American Mineralogist **75**, 656 (1990).
[3] D. G. Rancourt, M. Z. Dang and A. E. Lalonde, American Mineralogist **77**, 34 (1992).
[4] M. D. Dyar, American Mineralogist **78**, 665 (1993).
[5] G. B. Roger and S. F. Duncan, Hyperfine Interactions **91**, 571 (1994).
[6] D. L. Philips, J. Ass. Comput. Mach **9**, 84 (1962).
[7] S. Twomey, J. Ass. Comput. Mach **10**, 97 (1963).
[8] G. Le Caer and J. M. Dubois, J. Phys. E: Sci. Instrum **12**,

1083 (1979).
[9] C. Cordeiro, C. Diaz, F. Dominguez, and P. Miranda, Rev. Cub. Quim. **2**, 25 (1986).
[10] C. J. Koch, M. B. Madsen, and S. Morup, Surf. Sci. **156**, 249 (1985).
[11] F. van der Woude and A. J. Dekker, Phys. Stat. Sol. **18**, 181 (1966).
[12] C. Wivel and and S. Morup, J. Phys. E **14**, 605 (1981).
[13] S. Morup, J. Magn. Magn. Mat. **37**, 39 (1983).
[14] K. S. Baek, E. J. Hahn and H. N. Ok, Phys. Rev. B **36**, 763 (1987).
[15] V. I. Nikolaev and V. S. Rusakov, *Mössbauer investigation of ferrites*, Moscow State University, Moscow (1985).
[16] V. I. Nikolaev, V. S. Rusakov, and G. Yu. Fedina, *In Interaction of Mössbauer radiation with substance*, ed. R. N. Kuzmin, Moscow State University, Moscow (1985).